*Photocatalysis*
https://www.sciltp.com/journals/photocatalysis

**Supplementary Materials**

# Photocatalytic Oxidation of Cyclohexane in a Biphasic System Using Rapidly Synthesized Polymeric Carbon Nitride Films

Ayelet Tashakory, Venugopala Rao Battula * and Menny Shalom *

Department of Chemistry and Ilse Katz Institute for Nanoscale Science and Technology, Ben-Gurion University of the Negev, Beer-Sheva 8410501, Israel
* Correspondence: battula@bgu.ac.il (V.R.B.); mennysh@bgu.ac.il (M.S.)

## 1. Materials

All reagents and solvents were used as received from their respective commercial vendors, without further purification: melamine (99%), $Na_2SO_4$ (ACS reagent), potassium bromide (KBr), anhydrous, 99%, and (2,2,6,6-tetramethylpiperidin-1-yl)oxyl (TEMPO), 98+%, from Sigma-Aldrich; cyclohexane (HPLC isocratic grade) from Carlo Erba; cyclohexanone (technical) and cyclohexanol (technical) from BDH Chemicals; triethanolamine (TEOA, 99%) from Glentham, UK; sulfuric acid ($H_2SO_4$, 96% *w/w*, hydrochloric acid (HCl) 32% wt. (AR grade), and sodium chloride (NaCl), AR, from Bio-Lab; hydrobromic acid (HBr) 48% wt. (pure) from Acros; ascorbic acid, 99%, from Flurorochem; 2-propanol (IPA), ≥99.7% AR/ACS, from VWR chemicals; 1,5-dihydroxynaphthalene (1,5-DHN), 98%, from Angene.

Deionized water (18.2 MΩ cm resistivity at 25 °C, purified using a Millipore Direct-Q3 system) was used for all aqueous solutions preparation. Fluorine-doped tin oxide (FTO)-coated glass (12–14 Ω $sq^{-1}$) was purchased from Xop Glass company, Spain. Before use, the FTO was cut into rectangular pieces (1.3 cm × 2.5 cm) and sonicated with an aqueous detergent solution (Alconox, 1% m/v), ethanol, and acetone successively, for 15 min each, then dried in an air oven at 60 °C.

## 2. Synthesis

All synthetic protocols followed the procedures described by Tashakory et al.

### *2.1. Synthesis of Melem*

Melem (2,5,8-triamino-tri-s-triazine) was prepared via thermal condensation of melamine. Melamine was placed in a lidded ceramic crucible and heated in a muffle furnace under air to 400 °C at a rate of 5 °C $min^{-1}$. The temperature was maintained for 12 h, after which the furnace was allowed to cool naturally to room temperature. The resulting off-white bulk powder was then finely ground using a mortar and pestle.

### *2.2. Preparation of Supramolecular Assemblies*

Melem–melamine (Mel–M) supramolecular assembly with a molar ratio of 3:1, denoted as 3MelM, was prepared by mixing suitable quantities of melamine and melem, with a total mass of ~2 g (of both components), in 50 mL polypropylene centrifuge tubes with 45 mL of DI water. The suspension underwent sonication for 15 min, followed by shaking in an orbital shaker at 300 rpm for 24 h. The resulting mixture was centrifuged at 4500 rpm for 5 min, and the collected precipitate was dried in a vacuum oven for 24 h. The dried bulk material was ground into a fine powder for use in subsequent steps.

### *2.3. Preparation of Supramolecular Films ('Doctor-Blading')*

A paste was prepared by mixing 0.5 g of the 3MelM powder with 1 mL of ethylene glycol using a planetary centrifugal mixer (Thinky mixer, model ARV-310LED) equipped with a single 10 mm zirconia ball. The mixture

was homogenized at 1500 rpm for 5 min. The paste was then deposited onto FTO substrates using the doctor-blade deposition method, with a single layer of 3M Scotch Magic Tape 810 serving as a spacer to control the film thickness. The films were dried on a hot plate in a two-stage heating process: initially, the temperature was increased from room temperature to 60 °C at 5 °C $min^{-1}$ and held for 30 min. Subsequently, the temperature was raised to 85 °C for another 30 min, followed by natural cooling back to room temperature.

### *2.4. Synthesis of CN Films*

To synthesize CN films, two 3MelM films were stacked face-to-face and wrapped in aluminum foil, forming a sandwich structure. For samples labeled CN-M10 and CN-M20, an additional 0.1 g of melem powder was placed between the films. The sandwiched assemblies were then thermally treated in a tube furnace at 680 °C, yielding four types of CN films: CN-10, CN-20, CN-M10, and CN-M20. The numerical suffix represents the polymerization duration in minutes, while the "M" signifies the inclusion of melem powder; its absence indicates that no melem was present during calcination. After natural cooling to room temperature, the sandwiches were disassembled. In the CN-M10 and CN-M20 samples, excess CN powder (produced from the melem during calcination) was carefully removed using a scalpel before conducting photocatalytic tests.

### *2.5. Characterization*

X-ray diffraction (XRD) patterns were obtained using a PANalytical Empyrean diffractometer (equipped with an X'celerator position-sensitive detector) with a scanning time of ≈9 min for a $2\theta$ range of 5–60°, using Cu Kα radiation ($\lambda$ = 1.54178 Å), operation parameters: 40 kV, 30 mA. Fourier-transform infrared (FTIR) spectra were collected on a Thermo Scientific Nicolet iS5 using a diamond iD7 attenuated total reflectance (ATR) accessory. The chemical states of key elements were analyzed from X–ray photoelectron spectroscopy (XPS) measurements conducted on X-ray photoelectron spectrometer ESCALAB-Xi+ ultrahigh vacuum ($4 \times 10^{-10}$ bar) apparatus with an Al Kα X-ray source and a monochromator; all the binding energies in the XPS spectra were calibrated using the C 1s peak at 284.8 eV. The UV–vis diffuse reflectance spectrum (DRS, measured as %$R$) was measured using a Cary 100 spectrophotometer equipped with a diffuse reflectance accessory (DRA). To determine the absorbance spectrum of the CN-10 film a Kubelka-Munk function, $F(R)$, was calculated. The optical band gap ($E_g$) was determined using Tauc plot analysis, assuming a direct band gap. Photoluminescence (PL) spectrum was collected on a Horiba Scientific FluroMax 4 fluorimeter, with an excitation wavelength of $\lambda_{ex}$ = 380 nm. The morphology of the samples was characterized using a scanning electron microscopy (SEM, FEI VERIOS 460L) operated at 3.5 kV, 25 pA, or 5.0 kV, 50 pA using an Everhart–Thornley secondary electron detector; the samples were sputtered with 12 nm gold before analysis to avoid charging.

### *2.6. Photocatalytic Measurements*

Photocatalytic measurements were conducted using an 8-position DrySyn® OCTO Reaction Station, Asynt, UK, under 390 nm irradiation for 24 h. Each reaction tube contained 1 $cm^2$ CN film and 5 mL of solution. For biphasic reactions, 3.2 mL of the organic phase and 1.8 mL of the aqueous phase were used to maintain a total volume of 5 mL while ensuring proper contact between both phases and the CN film. Prior to irradiation, the solutions were purged with either $O_2$ or Ar gas for 20 min, transferred to the reaction station, and then purged again in the sealed headspace for an additional 20 min. The reaction temperature was maintained at 35 °C (unless stated otherwise for optimization studies) using a Huber Ministat 230 thermostat.

Scale-up experiments were performed under white LED illumination (100 W, $\lambda > 400$ nm) using 12 $cm^2$ CN-10 films in a total solution volume of 45 mL. Two systems were tested: pure cyclohexane (45 mL) and a biphasic mixture of cyclohexane (35 mL) and 1 M HCl (10 mL). The reaction tubes were purged with $O_2$ for 1 h prior to the start of the reaction and every 24 h thereafter. Samples were collected after 1, 2, 4, and 6 days for gas chromatography–mass spectrometry (GC–MS) analysis.

### *2.7. Product Analysis*

The reaction products were identified and quantified using a GC–MS system (Agilent 7890N GC coupled with an Agilent 5977A single-quadrupole mass-selective detector). GC chromatograms and MS spectra of main products can be found in the appendix at the end of the Supplementary Materials. Before analysis, each sample was filtered through a 0.22 µm syringe filter to remove any suspended CN particles. A 2 µL sample volume was injected for each run. Calibration curves for cyclohexanol and cyclohexanone in cyclohexane (peak area vs. concentration) were used to determine product concentrations.

In reactions involving an aqueous phase, the organic phase was first separated and dried over $Na_2SO_4$, then filtered as described above prior to GC–MS analysis.

## 3. Supplementary Figures

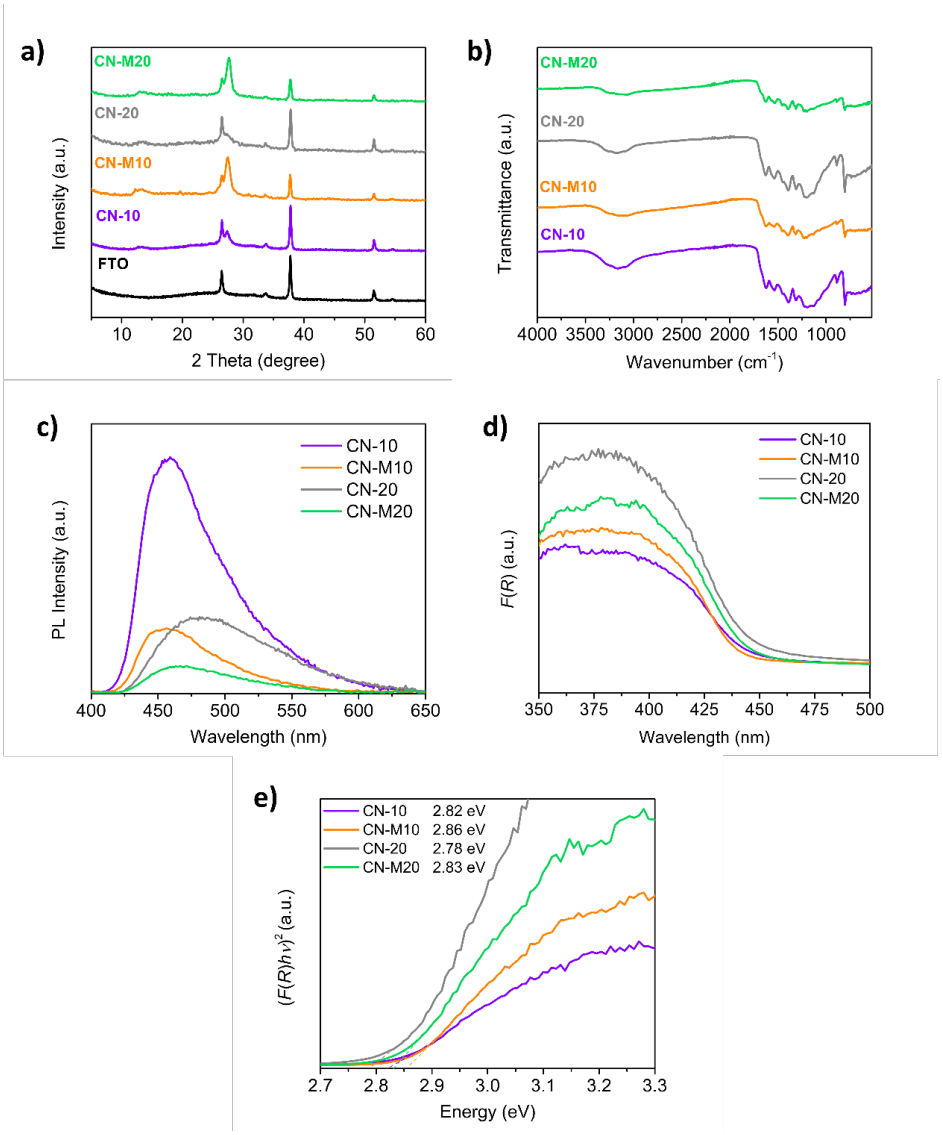


**Figure S1.** Structural and optical characterizations of CN-10, CN-M10, CN-20, and CN-M20 films. (**a**) X-ray diffraction (XRD) patterns; (**b**) Fourier-transform infrared (FTIR) spectra; (**c**) photoluminescence (PL) spectra; (**d**) F(R) spectra and (**e**) Tauc plot analyses.

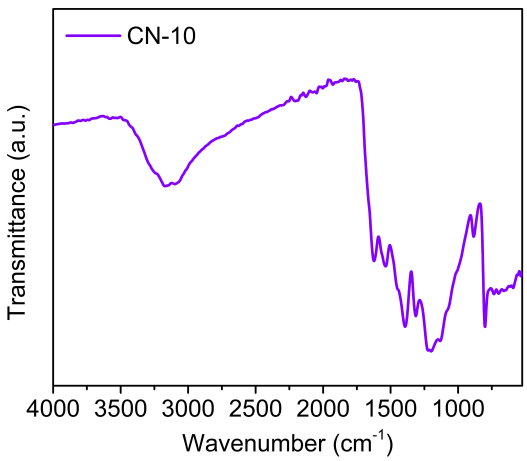


**Figure S2.** FTIR spectrum of CN-10.

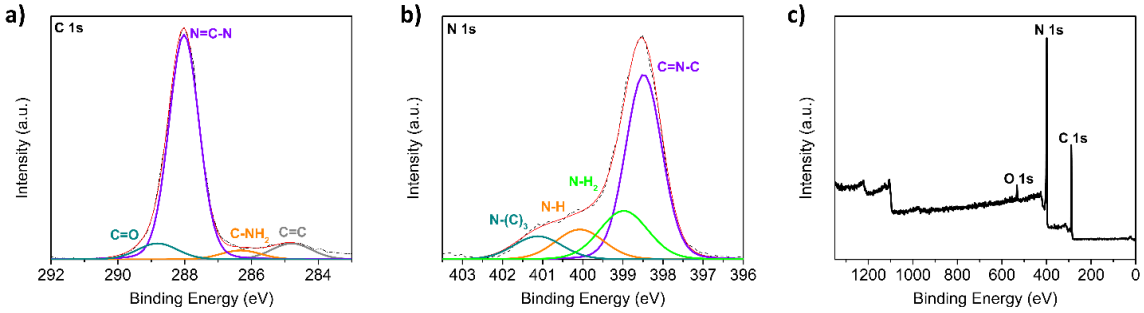


**Figure S3.** (**a**) C 1s; and (**b**) N 1s XPS spectra of the CN-10 film; (**c**) XPS survey spectrum.

**Table S1.** Elemental analysis of the CN-10 as was detected by XPS.

| | C (at. %) | N (at. %) | O (at. %) |
|---|---|---|---|
| CN-10 | 39.39 | 57.02 | 3.59 |

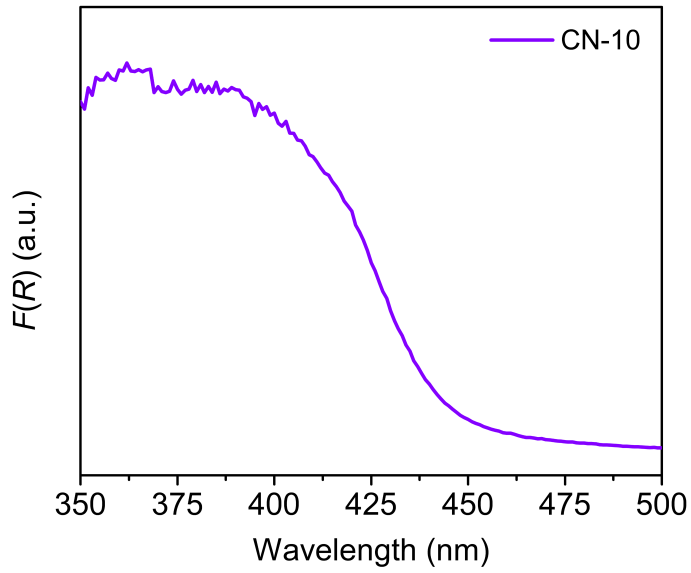


**Figure S4.** UV–vis diffuse reflectance spectra, presented as the Kubelka-Munk function, F(R), of CN-10.

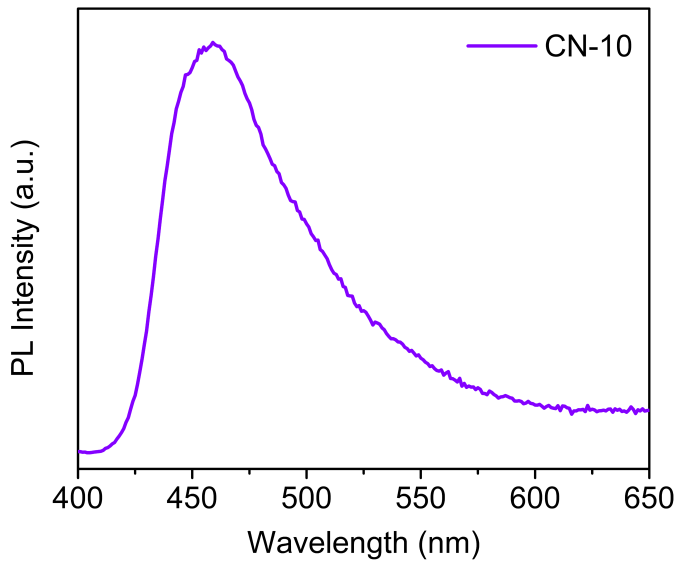


**Figure S5.** PL spectra of the CN films; $\lambda_{ex}$ = 380 nm.

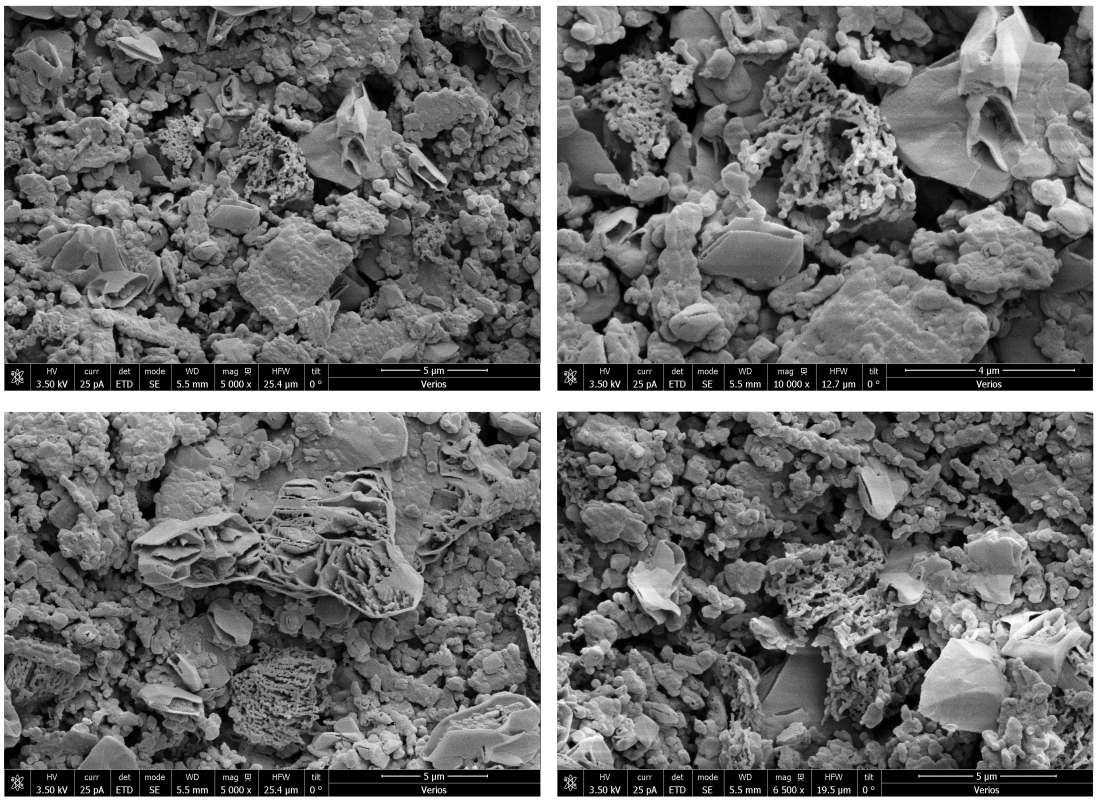

**Figure S6.** Additional top-view SEM images of CN-10.

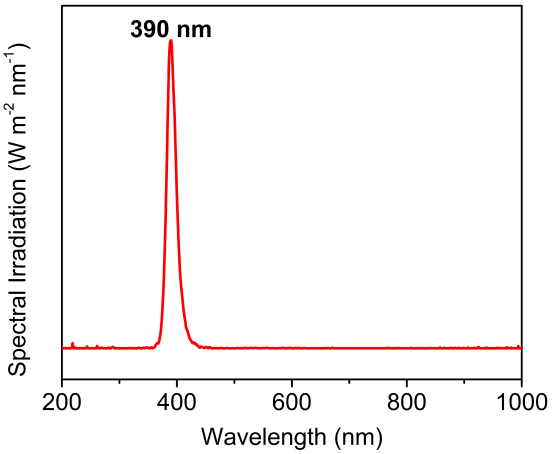


**Figure S7.** Multi-photoreactor light spectrum, irradiation wavelength is 390 nm.

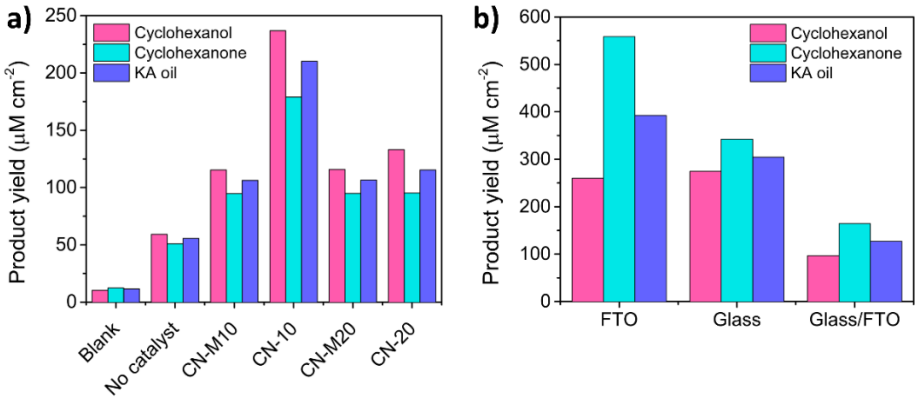


**Figure S8.** Optimization experiments of photocatalytic cyclohexane oxidation conditions. (**a**) Optimization of film; (**b**) Optimization of CN-10 substrate.

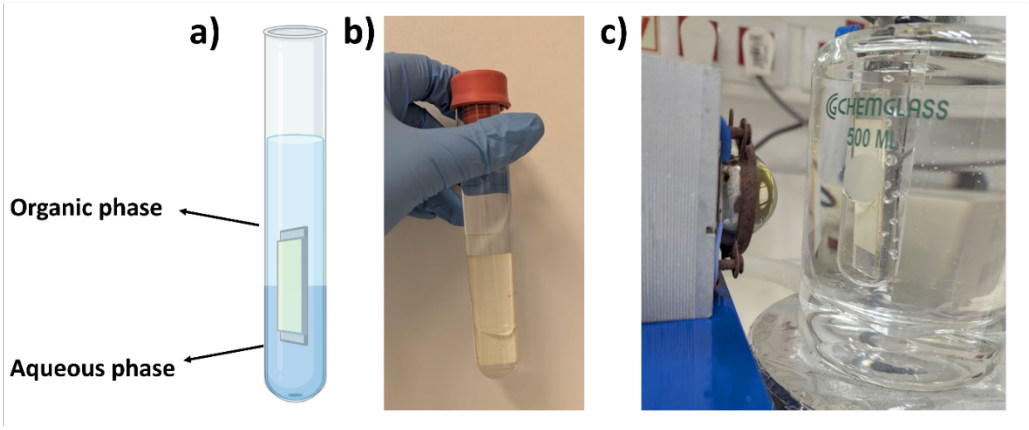


**Figure S9.** (**a**) an illustration; and (**b**) a digital picture of the biphasic aqueous-organic system; (**c**) The photocatalytic system, using white LED. The digital pictures were taken from the large-scale system.

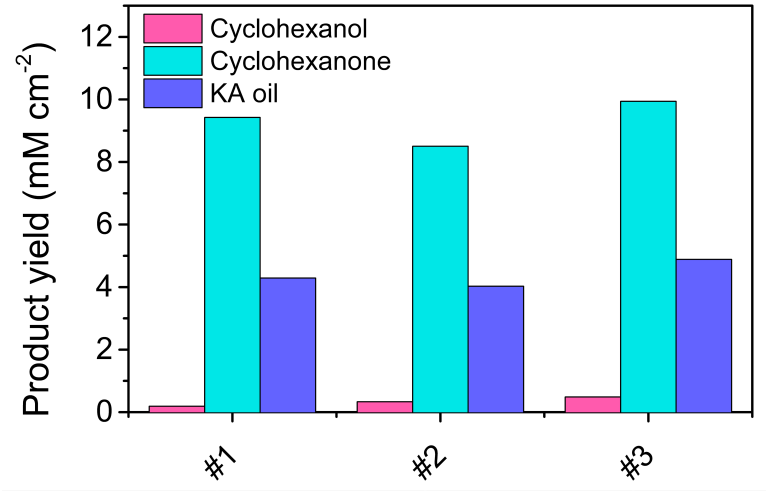


**Figure S10.** Reproducibility of the photocatalytic reaction, using CN-10 as the photocatalyst and adding 1 M HCl to the reaction.

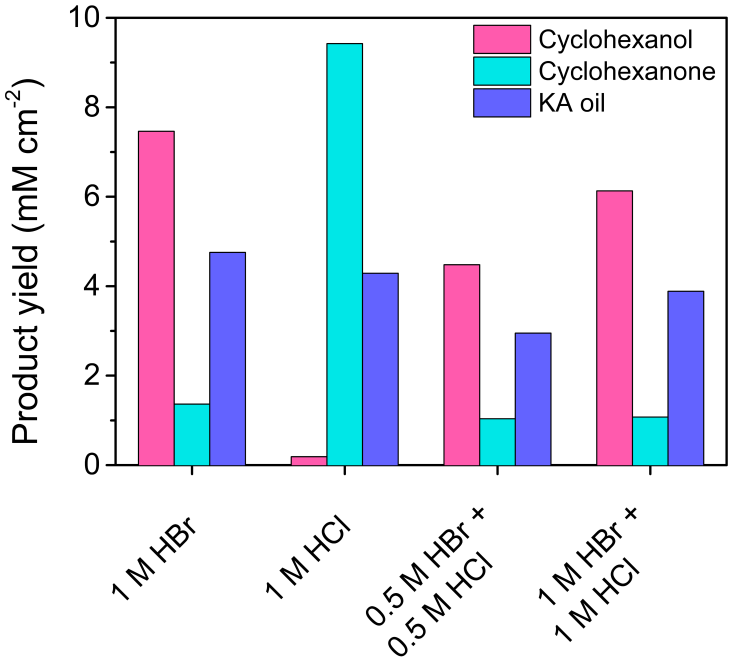


**Figure S11.** A comparison of product yield obtained in a biphasic system consisting of CHA with 1 M HBr, 1 M HCl, 1:1 mixture of 0.5 M HBr and 0.5 M HCl, and 1:1 mixture of 1 M HBr and 1 M HCl.

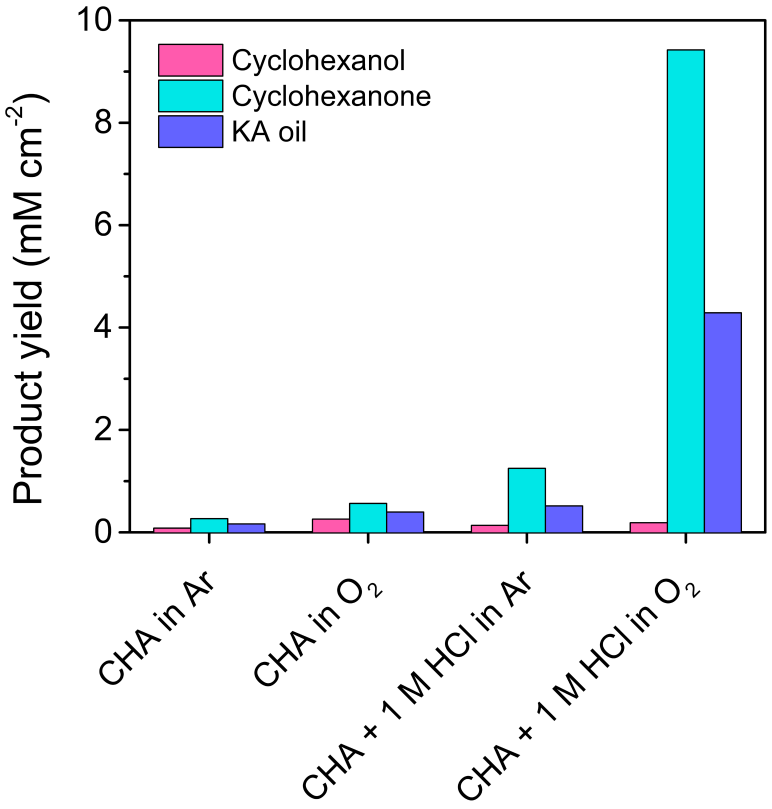


**Figure S12.** A comparison of product yield obtained in four different systems: pure CHA purged with Ar, pure CHA purged with $O_2$, biphasic system of CHA with 1 M HCl purged with Ar, and biphasic system of CHA with 1 M HCl purged with $O_2$.

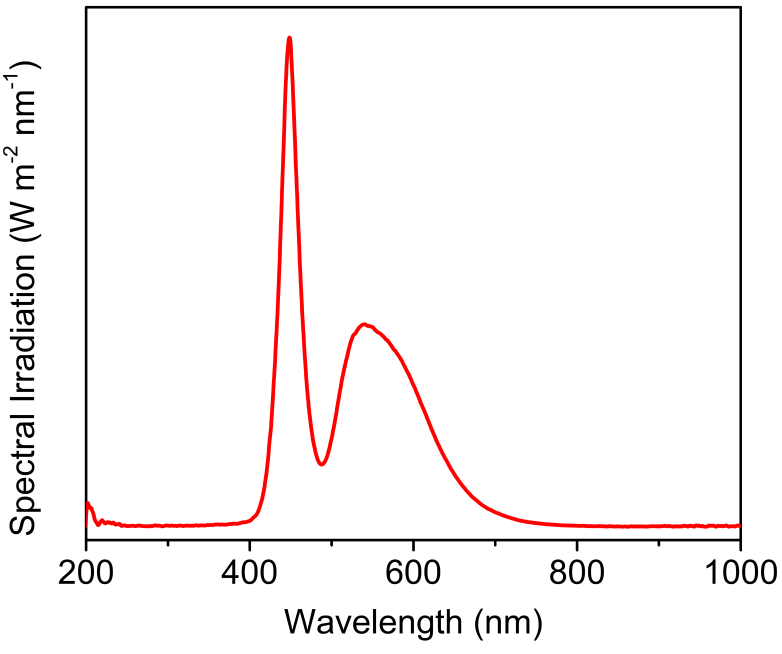


**Figure S13.** Irradiation spectrum of the 100 W, white LED used for the large-scale photocatalytic oxidation reactions.

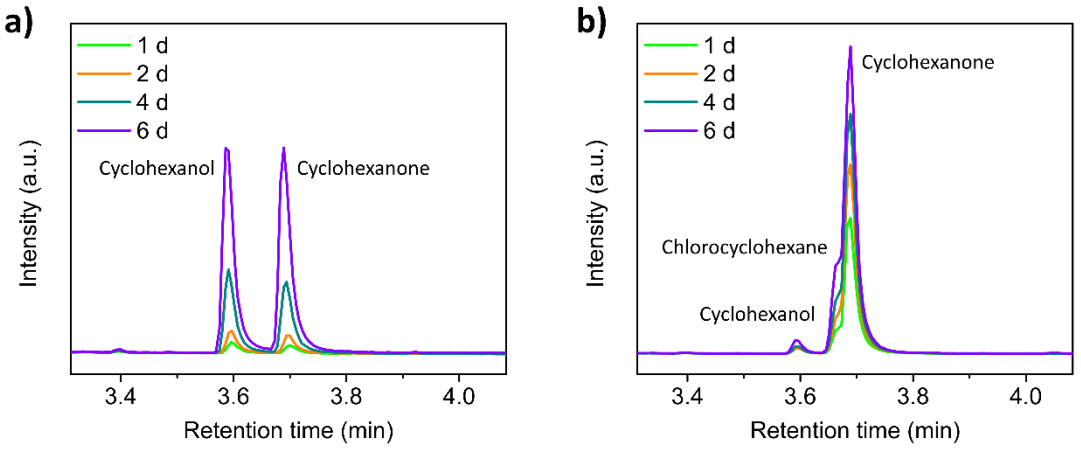


**Figure S14.** GC-MS curves showing the evolution of the major products in the large scale reactions: cyclohexanol, cyclohexanone and chlorocyclohexane in (**a**) pure CHA and (**b**) CHA + 1 M HCl.

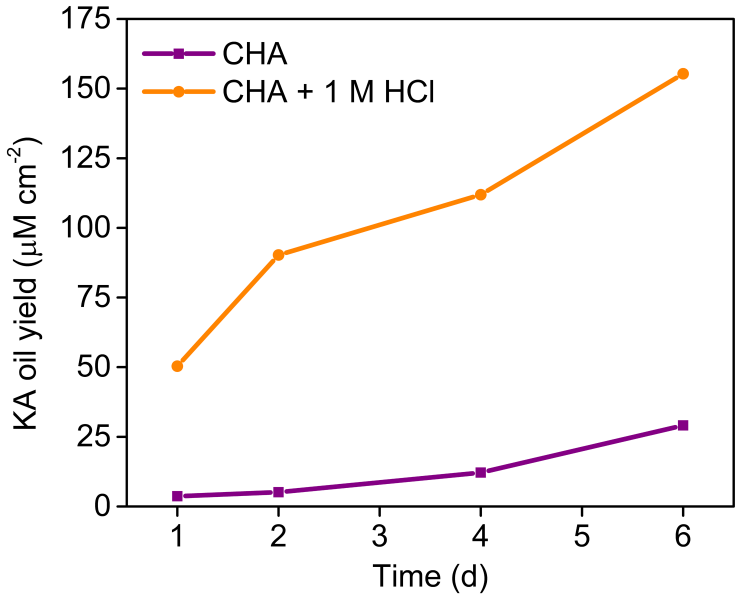


**Figure S15.** KA oil yield vs. time for pure CHA and the biphasic system consisting of CHA + 1 M HCl.

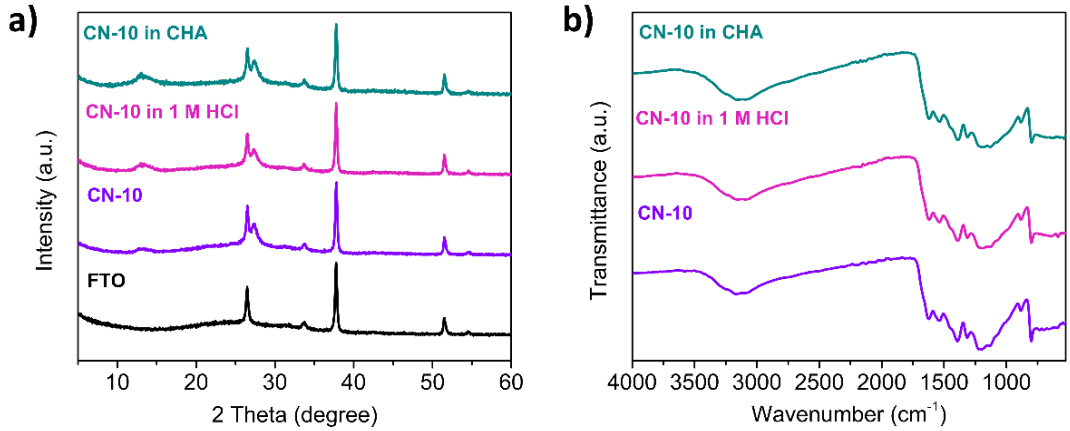


**Figure S16.** (**a**) XRD patterns and (**b**) FTIR spectra of pristine CN-10 film (purple) compared to used CN-film in the aqueous phase (pink) and organic phase (dark cyan) in the biphasic system.

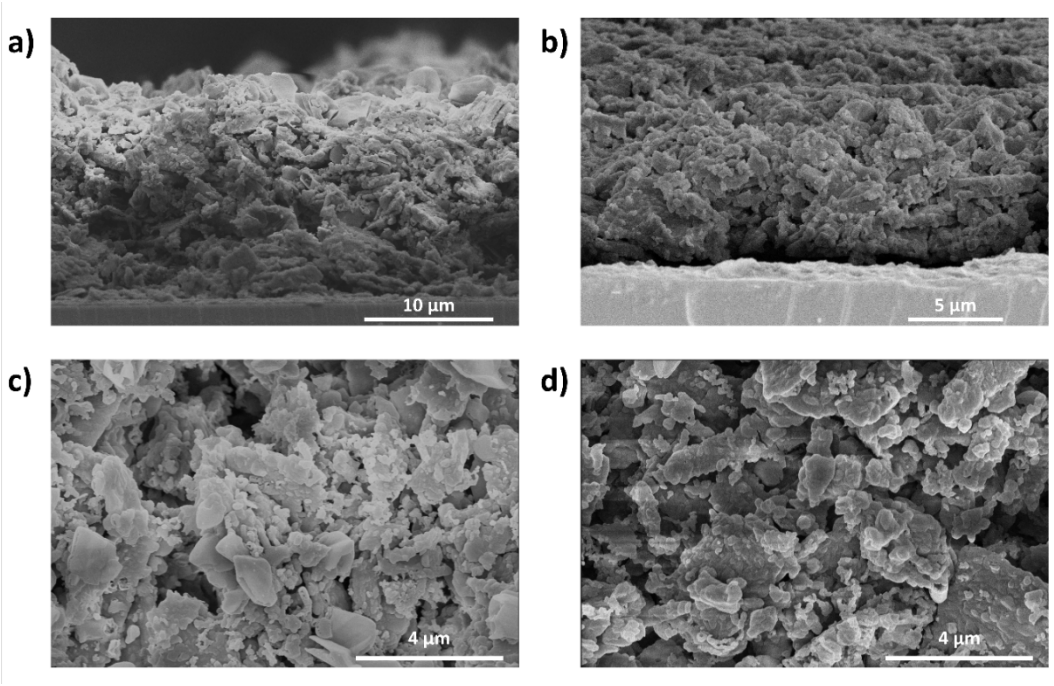


**Figure S17.** SEM imaging of the CN-10 film in (**a**,**c**) aqueous phase (1 M HCl) and (**b**,**d**) organic phase (CHA).

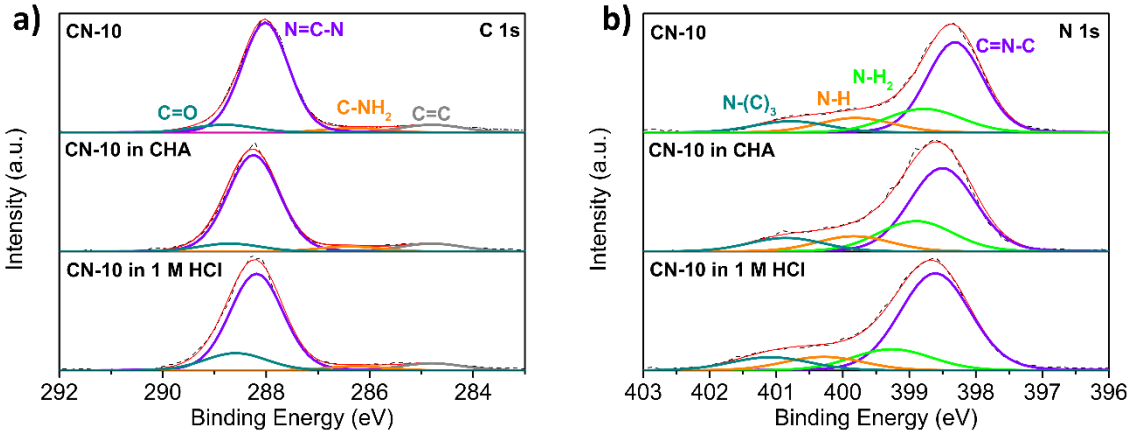


**Figure S18.** (**a**) C 1s and (**b**) N 1s spectra of the CN-10 film before and after the long-term photocatalytic measurements.

**Table S2.** XPS analysis of the CN-10 film elemental composition before and after the long-term photocatalytic reaction.

| | C (at. %) | N (at. %) | O (at. %) | Cl (at. %) |
|---|---|---|---|---|
| CN-10 | 39.39 | 57.02 | 3.59 | - |
| CN-10 in CHA | 41.1 | 53.09 | 4.82 | 0.99 |
| CN-10 in 1 M HCl | 40.25 | 54.97 | 4.23 | 0.54 |